2018 IEEE Intelligent Vehicles Symposium (IV)
Changshu, Suzhou, China, June 26-30, 2018

Path Tracking of Full Drive-by-Wire Electric Vehicle based on Model Prediction Control

Bing Zhang, Guoying Chen, Changfu Zong

***Abstract*—Developments of wire control and sensing technologies give more possibilities to automatic vehicle. For this, a path tracking controller is proposed to full drive-by-wire electric vehicle (FWEV). Method of model prediction control (MPC) is utilized to design path tracking controller, for ensuing dynamic stability with minimally sacrificing tracking performance, dynamic limit defined by stability phase plane is introduced as optimal constraints. Control method for realizing the desired motion with FWEV is designed subsequently. Finally, simulation results shown that this suggested path tracking controller can ensure the dynamic stability without compromising tracking accuracy.**

***Index Terms*—Path following, vehicle dynamic stability, phase plane， four-wheel independent steering, four-wheel independent driving.**

I. INTRODUCTION

In recent years, the automatic vehicle has attracted considerable attentions for its flexibility, convenience and safety[1]-[3], for this, intensive research has been done into the issues around it, and one of the most important things in this field is path-tracking problem, which is explained as tracking a given reference path [4],[6]. This is a complex task since the control law is required to guarantee tracking accuracy and safety synchronously [7].

Current researches focused on that problem have already achieved certain achievements. Paper [8] realized the vehicle path tracking by considering kinematic and dynamic control, and a MPC controller is introduced for dynamic controller. Pointed to the problem of trajectory control for independently driving vehicle, paper [9] changed the reference path to a form of corridor, which smoothed the steering motion as well as reduce the control effort. Paper [10] proposed vehicle path tracking method basing linear time-varying MPC, which introduced the linearized time-varying system constraints considered collision avoidance and human behavior. In paper [11], a curvature-based control method capable of both forward and backward path following is developed for off-axle hitching trailers.

*This project is supported by National Natural Science Foundation of China (Grant No. 51505178) and China Postdoctoral Science Foundation (Grant No.
2014M561289).

Author:Bing Zhang is with Department of State Key Laboratory of Automotive Simulation and Control, Jilin University, Changchun, China. (e-mail: zhangb0925@163.com)

Corresponding author: Guoying Chen is with Department of State Key Laboratory of Automotive Simulation and Control, Jilin University, Changchun, China. (e-mail: cgy-011@163.com)

Co-author:Changfu Zong is with Department of State Key Laboratory of Automotive Simulation and Control, Jilin University, Changchun, China. (e-mail: zongcf@jlu.edu.cn)

In general, most approaches attach importance to the safe trajectory acquisition, which is designed to avoid collision during following reference path, and the tracking accuracy should be ensured at the same time. However, the dynamic handling stability of vehicle is the essential foundation for safe driving during path following and cannot be ignored, and what is more important and difficult is that how to ensure the dynamic stability for vehicle body with minimal aggression to tracking performance. For this, pointing to the full drive-by-wire electric vehicle, (which is independently driven/braked and steered and has great advantages on automatic driving for its flexible dynamic characteristics), this paper systematically presents a control method for path tracking, which attaches most attention to ensure dynamic stability with minimal sacrifice of tracking accuracy. The scheme forementioned is applied basing on a hierarchical control structure introduced as Fig. 1, which mainly contains six layers: the first layer is identification and estimation layer which used to obtain the vehicle states as well as environment datas; the second layer is trajectory planning layer that achieve the optimal driving path according current traffic environment; the third layer is the path tracking layer which is key point in this paper, this layer is designed by MPC method and utilized to achieve the desired motion confirm to the reference path, additional, the dynamic stability constraint based phase plane is introduced to this layer for guaranteeing vehicle stability; sequentially, the last three layers are presented to realize the tracking motion with FWEV, and they are functionally divided into motion control (MC) layer, control allocation (CA) layer and executive layer.

This paper mainly describes the path tracking control and the tracking motion realization for FWEV, which enclosed by red solid-line in Fig. 1. And the structure described as follows: Sec. Ⅱ describes both single track and double track vehicle dynamic models used in controller. Sec. Ⅲ tells about the design of path tracking controller considered the dynamic stability constraints. The realization for motion desired is illustrated in Sec. Ⅳ, which contains MC layer, CA layer and executive layer. The simulation results are shown in Sec. Ⅴ. Finally, a short summary and an outlook are given in the concluding Sec. Ⅵ.

II. DYNAMIC MODELS FOR CONTROLLER

A. Single Track Model for Path Tracking

In the path tracking layer, the controller is tend to track the reference path according to a traditional vehicle character, here, the single track model with 2-DOF serves as a reference model for path tracking layer to keep the vehicle handling characteristics easy to manoeuvre, as shown by (1), which consisted of three velocity states and two position states.

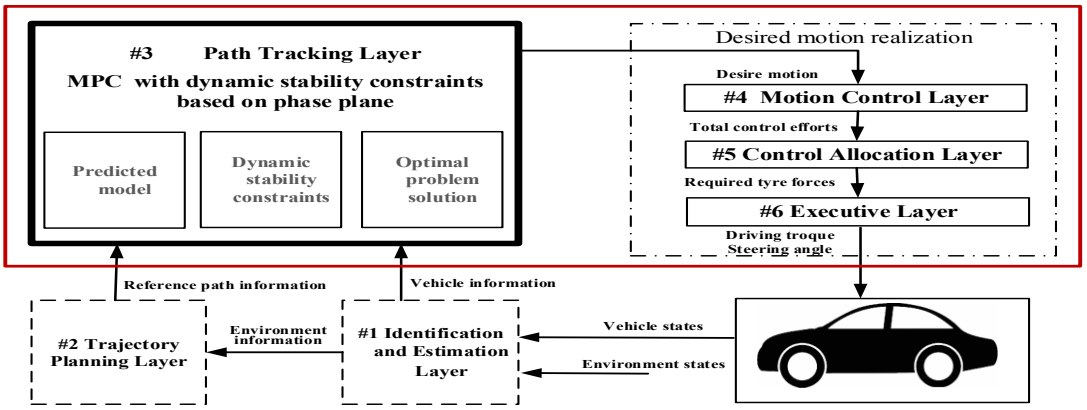

Figure 1. Hierarchical control structure.

$$\begin{cases} m\dot{V}_y = -mV_x\dot{\psi} + 2[C_{\alpha f}(\delta_f - \dfrac{V_y + l_f\dot{\psi}}{V_x}) + C_{\alpha r}\dfrac{l_r\dot{\psi} - V_y}{V_x}] \\ I_z\ddot{\psi} = 2[l_f C_{\alpha f}(\delta_f - \dfrac{V_y + l_f\dot{\psi}}{V_x}) - l_r C_{\alpha r}\dfrac{l_r\dot{\psi} - V_y}{V_x}] \\ \dot{Y} = \dot{x}\sin\varphi + \dot{y}\cos\varphi \\ \dot{X} = \dot{x}\cos\varphi - \dot{y}\sin\varphi \\ \dot{\beta} = \dfrac{C_{\alpha f} + C_{\alpha r}}{mV_x}\beta + (\dfrac{l_f C_{\alpha f} - l_r C_{\alpha r}}{mV_x^2} - 1)\dot{\psi} - \dfrac{C_{\alpha f}}{mV_x}\delta_f \end{cases} \quad (1)$$

Where X is the vehicle longitudinal position, and Y is the vehicle lateral position. $C_{\alpha f}$ and $C_{\alpha r}$ are the equivalent corner stiffness. For studying the stability in phase plane consisted of sideslip angle and sideslip rate, the model is arranged as

$$\begin{cases} \ddot{\psi} = \dfrac{M_z}{I_z} = \dfrac{(l_r C_{\alpha r} - l_f C_{\alpha f})}{I_z}\beta - \dfrac{l_f^2 C_{\alpha f} + l_r^2 C_{\alpha r}}{V_x I_z}\dot{\psi} + \dfrac{l_f C_{\alpha f}}{I_z}\delta_f \\ \dot{\beta} = \dfrac{F_y}{mV_x} - \dot{\psi} = -\dfrac{C_{\alpha f} + C_{\alpha r}}{mV_x}\beta + (\dfrac{l_f C_{\alpha f} - l_r C_{\alpha r}}{mV_x^2} - 1)\dot{\psi} \\ \qquad + \dfrac{C_{\alpha f}}{mV_x}\delta_f \end{cases} \quad (2)$$

Where, F_y is total lateral force; ψ is the yaw angle; V_x and V_y are the longitudinal and lateral velocities of the vehicle; And the vehicle sideslip angle β can be expressed as

$$\beta = \frac{V_y}{V_x} \quad (3)$$

For reducing computation complexity and improving control facilitation, model (1) is linearized to format of

$$\begin{cases} \dot{x} = Ax(t) + Bu(t) \\ y = Cx \end{cases} \quad (4)$$

Meanwhile, the vehicle state of x is chosen as $[V_x, V_y, \psi, \dot{\psi}, Y, X, \beta]^T$, control input u is δ_f, which is the front steering angle desired, and system output $y = [\psi, Y]$.

B. Double Track Model for FWEV

For accurately realizing the desired motion with FWEV, a double-track model with 3-DOF in Fig. 2. is introduced to feature its dynamic characteristics, which has ignored the

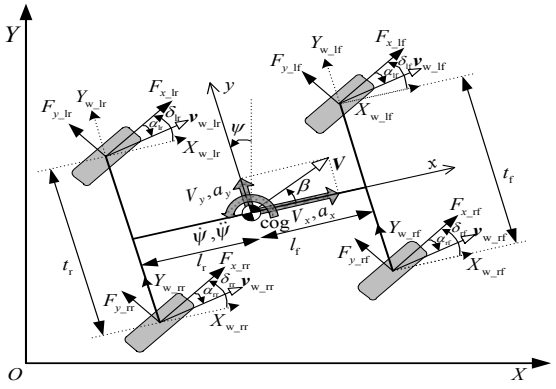

Figure 2. Double track model.

vertical and pitch motion. The dynamic equations are given as (5)

$$\begin{cases} a_x = \dot{V}_x - \dot{\psi}V_y = \dfrac{1}{m}\left(\sum_{i=1}^{r}\sum_{j=f}^{r} X_{w\_ij} - \dfrac{1}{2}C_D A_f \rho_0 V_x^2\right) \\ a_y = \dot{V}_y + \dot{\psi}V_x = \dfrac{1}{m}F_y = \dfrac{1}{m}\sum_{i=1}^{r}\sum_{j=f}^{r} Y_{w\_ij} \\ M_z = I_z\ddot{\psi} = \dfrac{t_f}{2}\left(X_{w\_rf} - X_{w\_lf}\right) + \dfrac{t_r}{2}\left(X_{w\_rr} - X_{w\_lr}\right) \\ \qquad + l_f\left(Y_{w\_lf} + Y_{w\_rf}\right) - l_r\left(Y_{w\_lr} + Y_{w\_rr}\right) \end{cases} \quad (5)$$

The resultant longitudinal and lateral tyre force X_{w_ij} and Y_{w_ij} are given by

$$\begin{cases} X_{w\_ij} = F_{x\_ij}\cos\delta_{ij} - F_{y\_ij}\sin\delta_{ij} \\ Y_{w\_ij} = F_{x\_ij}\sin\delta_{ij} + F_{y\_ij}\cos\delta_{ij} \end{cases}, \forall i \in \{l,r\}, \forall j \in \{f,r\} \quad (6)$$

Where F_{x_ij} and F_{y_ij} are given by longitudinal and lateral tyre force referred to wheel coordinate system, δ_{ij} represents the wheel steering angle.

C. Tyre Model

For realizing the computed tyre forces, relation between tyre sideslip angle and tyre forces is explained by employing tyre model in [12], given by

$$F_{y\_ij} = -C_{\alpha\_ij}\sqrt{1 - \left(\frac{F_{x\_ij}}{\mu_{ij}F_{z\_ij}}\right)^2}\frac{\mu_{ij}}{k_{ij}}\tan^{-1}\left(\frac{k_{ij}}{\mu_{ij}}\alpha_{ij}\right) \quad (7)$$

Where $k_{ij} = C_{\alpha\_ij}\pi / pF_{z\_ij}$, and C_{α_ij} is the tyre cornering stiffness. p is the curve-fitting constant which set as '2.9' in this paper, and the angle σ_{ij} between velocity of wheel center and the longitudinal axle of vehicle body is defined as

$$\sigma_{ij} = \alpha_{ij} + \delta_{ij} \quad (8)$$

and computed by

$$\begin{cases} \sigma_{\mathrm{lf,rf}} = \tan^{-1}\left(\left(V_y + l_{\mathrm{f}}\dot{\psi}\right)\Big/\left(V_x \mp t_{\mathrm{f}}\dot{\psi}/2\right)\right) \\ \sigma_{\mathrm{lr,rr}} = \tan^{-1}\left(\left(V_y - l_{\mathrm{r}}\dot{\psi}\right)\Big/\left(V_x \mp t_{\mathrm{r}}\dot{\psi}/2\right)\right) \end{cases} \quad (9)$$

III. PATH TRACKING CONTROLLER CONSIDERED DYNAMIC STABILITY

The path tracking layer's primary task is accurately following reference path and synchronously ensuring vehicle dynamic stability. With these objectives met, it is desirable to minimally invasive to tracking performance while avoiding vehicle unstability. For above, the path tracking controller with method of model prediction control is designed with objective of minimizing the error between vehicle actual path and the given reference path, furthermore, the stable boundary based on phase plane is introduced as inequality constraint to the optimal problem for guaranteeing the dynamic stability.

A. Stable Boundary Identification based on Phase Plane

For stable operating of path tracking, the controller confines the states of the vehicle to remain within a stable handling boundary in phase plane comprised by vehicle sideslip angle and sideslip angle speed. Since the longitudinal velocity and friction factor have important influence on stable handling boundary [13],[14], in this paper, the model (2) combined with (7) is established in MATLAB/Simulink, and the stable boundary is studied with different initial point of $(\beta, \dot{\beta})$ under different conditions decided by longitudinal vehicle velocity and friction factor. A set of curves under single condition in phase plane is typically shown in Fig. 3, where the stable boundary is marked as red lines. The dynamic handling stability region is ascertained with

$$\left|\beta + E_1\dot{\beta}\right| \le E_2 \quad (10)$$

Meanwhile, parameters E_1 and E_2 are interpolation functions of velocity V_x and friction factor μ.

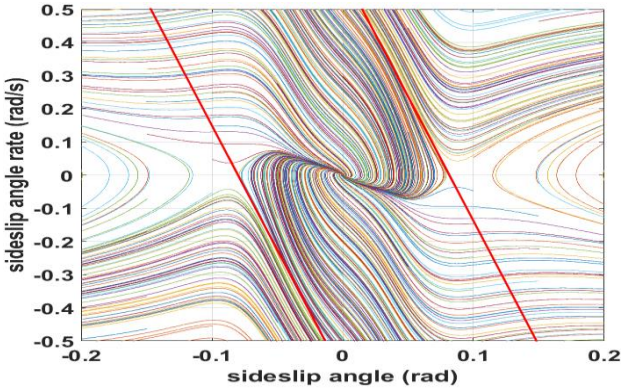

Figure 3. Stability boundary in $\beta - \dot{\beta}$ phase plane.

And according to equation (2) and (10), the dynamic stability constraints for control input at each time step k, which ensures dynamic stability is

$$H_{stab}u(\mathrm{k}) + \mathrm{G}_{stab}\,x(\mathrm{k}) \le E_2 \quad (11a)$$

$$-(H_{stab}u(\mathrm{k}) + \mathrm{G}_{stab}\,x(\mathrm{k})) \le E_2 \quad (11b)$$

B. MPC Controller with Dynamic Stability Constraint

For limiting control effort, the output of MPC controller is increment Δu, and the control objectives outlined previously can be expressed as the following receding horizon optimal control problem.

$$\begin{aligned} \min: J = &\sum_{i=1}^{Np}\left\|Y_{ref}(k+i|k) - Y_{sys}(k+i|k)\right\|_Q^2 \\ &+ \sum_{i=1}^{Nc-1}\left\|\Delta u(k+i|k)\right\|_R^2 + \rho\varepsilon^2 \end{aligned} \quad (12a)$$

$$s.t. \qquad \Delta U_{\min} \le \Delta U \le \Delta U_{\max} \quad (12b)$$

$$U_{\min} \le U \le U_{\max} \quad (12c)$$

$$Y_{\min} - \varepsilon \le Y_{sys} \le Y_{\max} + \varepsilon \quad (12d)$$

$$H_{stab}u(\mathrm{k}+1) + \mathrm{G}_{stab}\,x(\mathrm{k}+1) \le E_2 \quad (12e)$$

$$-(H_{stab}u(\mathrm{k}+1) + \mathrm{G}_{stab}\,x(\mathrm{k}+1)) \le E_2 \quad (12f)$$

Where N_p and N_c are the prediction and control horizons respectively. The first section in the objective function (12a) represents the tracking objective, thus, error between the solution trajectory and the desired linear behavior is penalized through a weighted norm, which is utilized to optimize the control input to minimize the tracking error. In this paper, the input for path tracking controller is set as δ_f, but since the restrictions of the actuators, the control variable of MPC controller is defined as increment $\Delta\delta_f$. the second term of (12a) is introduced for minimizing control effort. And the final term in of (12a) is a penalty on the slack variables, which is employed to ensure the feasibility under strict constraints. The dynamic constraints (12b)-(12d) describe the constraints for the control value according to the limit of system output and actuator. Constraints of (12e) and (12f) limit the vehicle maneuvered within a dynamic stable handling region, and this paper only limit the stability of the step next to current time. The first control increment is utilized to the system as

$$u(k+1) = u(k) + \Delta u(k+1) \quad (13)$$

In this paper, the desired longitudinal velocity is a certain constant pre-input to the path tracking layer from trajectory planning layer, and for suppressing sideslip motion to the minimum level for stable purpose, the desired lateral velocity should be '0'. According the desired front steering angle δ_f achieved by MPC controller, the desired yaw speed is defined as

$$\dot{\psi}_{\mathrm{d}} = \frac{V_x/(l_{\mathrm{f}} + l_{\mathrm{r}})}{1 + K_{\mathrm{g}}V_x^2}\cdot\delta_{\mathrm{f}} \quad (14)$$

Where K_g is the understeer degree. With the desired longitudinal and lateral velocities given by

$$V_{xd} = V_{x0} + \int_0^t a_{xd}(\tau)\,d\tau \qquad (15)$$

$$V_{yd} = 0 \qquad (16)$$

IV. REALIZATION OF TRACKING MOTION FOR FULL DRIVE-BY-WIRE VEHICLE

For realizing desired motion forementioned, MC layer firstly changes the desired vehicle motion to total efforts of vehicle, which are subsequently decomposed to eight tyre forces in CA layer, which are followed and actualized by actuator in executive layer.

A. Motion Controller

For achieving the desired motion and decoupling the relation between direction of longitudinal, lateral and yaw, techniques of SMC (sliding mode control) and TSMC (terminal sliding mode control) are employed here, which used to the achieved total vehicle efforts by:

$$\begin{cases} F_{xd} = m\left(-V_y\dot{\psi} + \dfrac{C_D A_f \rho_0 V_x^2}{2m} + a_{xd} - \eta_{1n}\,\mathrm{sat}(s_1/\phi_1)\right), \{F_{xd} \mid |F_{xd}| \le \mu m g\} \\ F_{yd} = m\left(V_x\dot{\psi} - \eta_{2n}\,\mathrm{sat}(s_2/\phi_2)\right), \{F_{yd} \mid |F_{yd}| \le \mu m g\} \\ M_{zd} = I_z\left\{(a_x + V_y\dot{\psi})\left(\dfrac{\delta_f/(l_f+l_r)}{1+K_g V_x^2} - \dfrac{2K_g V_x^2 \delta_f/(l_f+l_r)}{(1+K_g V_x^2)^2}\right)\right. \\ \left. + \dfrac{V_x\dot{\delta}_f/(l_f+l_r)}{1+K_g V_x^2} + \dfrac{\alpha_3 q_3}{\beta_3 p_3}(\dot{\psi}-\dot{\psi}_d)^{2-p_3/q_3}\left(\dfrac{-\alpha_{3n}s_3 - \beta_{3n}s_3^{q_{3n}/p_{3n}}}{\alpha_3(\dot{\psi}-\dot{\psi}_d)} - 1\right)\right\} \end{cases} \qquad (17)$$

Where p_3 and q_3 are positive odd numbers and $1 < p_3/q_3 < 2$. s_1, s_2 and s_3 are the slid mode surface defined in paper [15], and the function of *sat* is defined as

$$sat\left(\frac{s_k}{\phi_k}\right) = \begin{cases} s_k/\phi_k & \text{if } |s_k| < \phi_k \\ \mathrm{sgn}(s_k/\phi_k) & \text{if } |s_k| \ge \phi_k \end{cases} \qquad (18)$$

B. Tyre Force Allocation

In CA layer, the tyre forces are achieved by solving an optimal problem as

$$\min: \quad J_{CA} = \sum_{i=1}^{r}\sum_{j=f}^{r} \frac{X_{w\_ij}^2 + Y_{w\_ij}^2}{\mu_{ij}^2 F_{z\_ij}^2} \qquad (19a)$$

$$\text{s.t.} \quad A_{\lim} u_{CA} \le b_{\lim} \qquad (19b)$$

$$A_{eq} u_{CA} = b_{eq} \qquad (19c)$$

where $u_{CA} = \left[X_{w\_lf} \;\; X_{w\_rf} \;\; X_{w\_lr} \;\; X_{w\_rr} \;\; Y_{w\_lf} \;\; Y_{w\_rf} \;\; Y_{w\_lr} \;\; Y_{w\_rr}\right]^T$ and represents the vector consisted of eight tyre forces in Fig. 1.

Cost function of (19a) is the square sum of workloads of four wheels, which is employed to maximize the safety margin. (19b) integratively describes the tyre stability limit referred to stability friction circle linearized in [15], and defined as

$$\begin{aligned} &-\mu_{ij}F_{z\_ij} < X_{w\_ij} < \mu_{ij}F_{z\_ij}, \\ &-\mu_{ij}F_{z\_ij} < Y_{w\_ij} < \mu_{ij}F_{z\_ij}, \\ &-\sqrt{2}\mu_{ij}F_{z\_ij} < X_{w\_ij} + Y_{w\_ij} < \sqrt{2}\mu_{ij}F_{z\_ij}, \\ &-\sqrt{2}\mu_{ij}F_{z\_ij} < Y_{w\_ij} - X_{w\_ij} < \sqrt{2}\mu_{ij}F_{z\_ij} \end{aligned} \qquad (20)$$

Where F_{z_ij} is the tyre vertical load and refer to [15]. The coefficient in (19c) is limited to achieve desired total effort according (5) and (17).

C. Executive Layer

Executive layer is designed for realizing the tyre forces achieved in CA layer. Since the small control region of tyre sideslip angle α_{ij}, we can assume $\delta_{ij} \approx \sigma_{ij}$, therefore the tyre forces are achieved as

$$\begin{cases} F_{y\_ij} \approx -X_{w\_ij}\sin\sigma_{ij} + Y_{w\_ij}\cos\sigma_{ij} \\ F_{x\_ij}^* = X_{w\_ij}\cos\sigma_{ij} + Y_{w\_ij}\sin\sigma_{ij} \end{cases} \qquad (21)$$

where the longitudinal tyre forces is achieved by estimating.

And by the tyre model described in equation (7), the sideslip angle can be computed by

$$\alpha_{ij} = -\frac{\mu_{ij}}{k_{ij}}\tan\left\{\frac{k_{ij}}{\mu_{ij}}\cdot\frac{F_{y\_ij}}{C_{\alpha\_ij}\sqrt{1-\left(F_{x\_ij}^*\cos 22.5^\circ/\mu_{ij}F_{z\_ij}\right)^2}}\right\} \qquad (22)$$

Then the steering angle of the wheel δ_{ij} is obtained by

$$\delta_{ij} = \sigma_{ij} - \alpha_{ij} \qquad (23)$$

And the traction/braking force and torque of each wheel are obtained by

$$F_{x\_ij} = X_{w\_ij}\cos\delta_{ij} + Y_{w\_ij}\sin\delta_{ij} \qquad (24)$$

$$T_{w\_ij} = J_{w\_ij}\dot{\omega}_{w\_ij} + F_{x\_ij}R_{w\_ij} + T_{b\_ij} \qquad (25)$$

V. RESULT AND DISCUSSIONS

The controller is set up in MATLAB/Simulink, with a FWEV model provided by CarSim. The primary parameters are listed in table1.In this section, the simulation is implemented by tracking a double-change-lane, which reference output is shown as equation (26), and the proposed controller (SCC) is compared with the traditional controller without considering the stability constraints (NSCC). The simulation is under different sets of driving conditions decided by longitudinal vehicle speed and friction coefficient. In the first set of simulation, the longitudinal speed is kindly set as 30 kilometers per hour, and the road condition is set as a high friction with parameter of 0.9. And the second set of the simulation is set the longitudinal speed as 80 kilometers per hour and the friction factor is 0.5, which is more severe than the previous. Finally, the simulation is done with a varied speed, which is climb from 30 to 120 kilometers per hour in 20 seconds, with the friction factor 0.4.

$$\begin{aligned} Y_{ref}(X) &= \frac{d_{y1}}{2}(1+\tanh(z_1)) - \frac{d_{y2}}{2}(1+\tanh(z_2)) \\ \psi_{ref}(X) &= \tan^{-1}\left(d_{y1}\left(\frac{1}{\cosh(z_1)}\right)^2\left(\frac{1.2}{d_{x1}}\right) - d_{y2}\left(\frac{1}{\cosh(z_1)}\right)^2\left(\frac{1.2}{d_{x2}}\right)\right) \end{aligned} \qquad (26)$$

Where $z_1 = 2.4(X - 27.19)/25 - 1.2$, $z_2 = 2.4(X - 56.46)/21.95 - 1.2$.

TABLE I. VEHICLE PARAMETER USED IN SIMULATION

Symbol	Value and Unit
m	1723 kg
I_Z	4175 kgm^2
l_f	1.232 m
l_r	1.468 m
$C_{\alpha f}$	62900 N/rad
$C_{\alpha r}$	62700 N/rad

Fig. 4 shows that the controller with dynamic stability constraints shows the similar tracking and dynamic stability performance to the NSCC controller during gentle driving condition, which explains that the proposed controller ensures the dynamic stability without compromising to the tracking performance.

Fig. 5 shows that during more severe condition, comparing with vehicle operated by NSCC, the vehicle operated by proposed controller stays within a dynamic stable region.

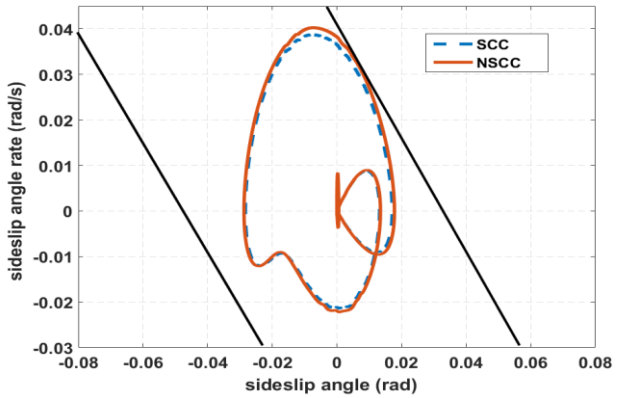

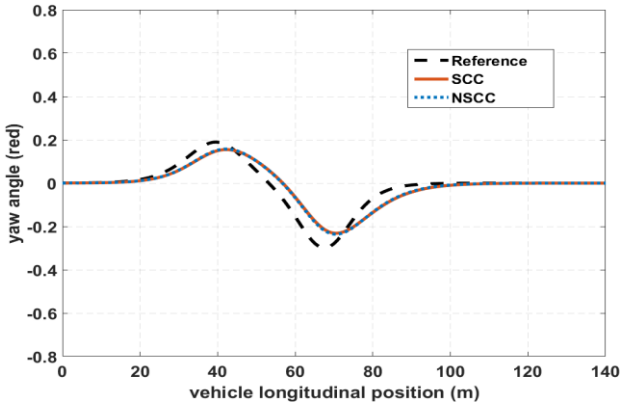

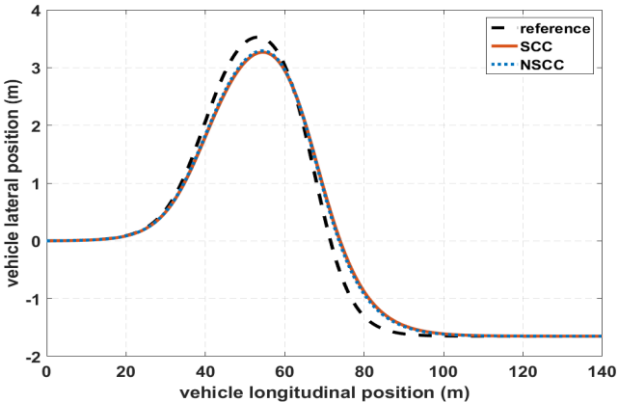

Figure 4. μ =0.9, V_x =30km/h

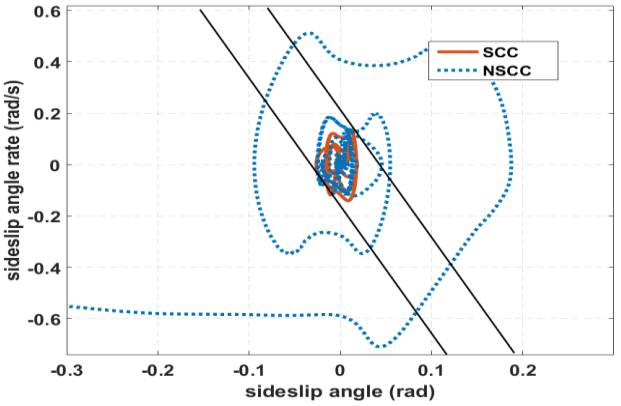

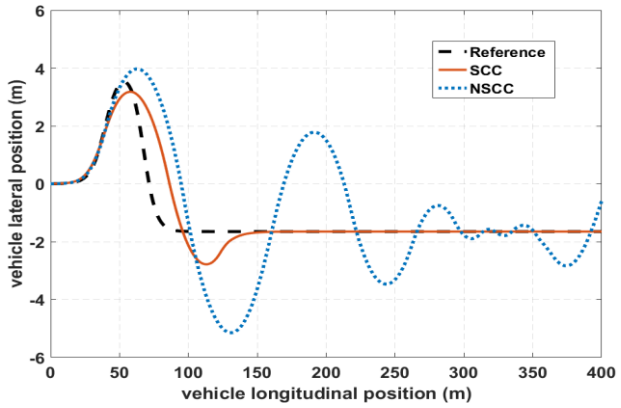

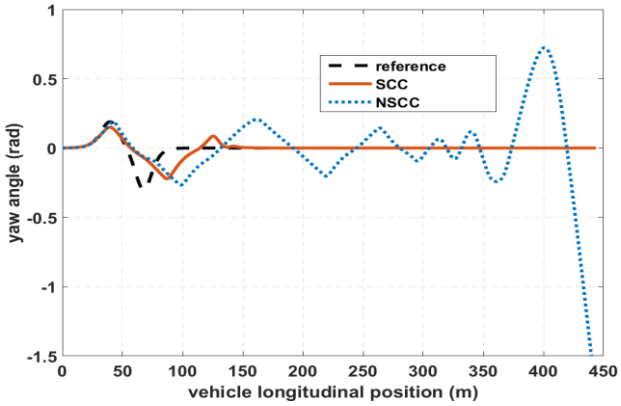

Figure 5. μ =0.5, V_x =80 km/h

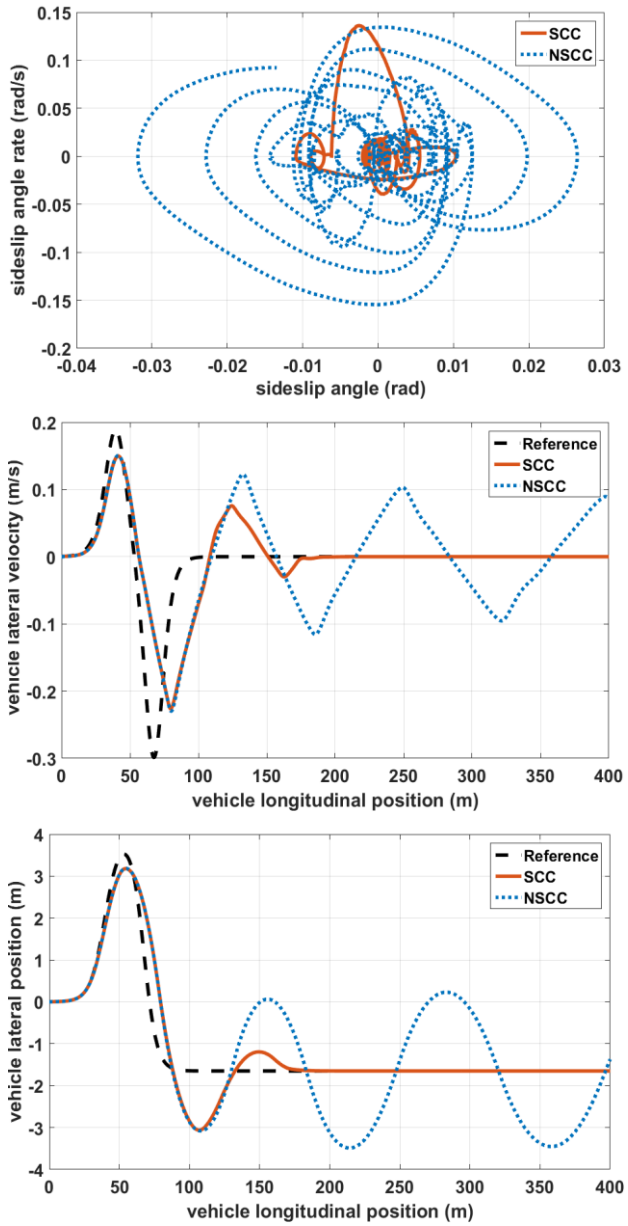

Figure 6. Variable velocity, μ =0.4

Furthermore, Fig. 6 gives the simulation results during variable velocity condition. It can be observed that as the vehicle longitudinal velocity increasing, vehicle controlled by NSCC can't coverage to stable point over time, contrarily, the SCC can control the vehicle within the dynamic stable region and finally return to stable point.

Additionally, from each simulation, it can be discovered that introduction of dynamic stable constraints will rarely influences the path tracking accuracy, which adheres to the purpose of ensuring the dynamic stability with minimally sacrificing the tracking performance.

VI. Conclusion

Facing the problem of both tracking performance and dynamic stability in path tracking, this paper presented an efficient trajectory tracking algorithm for full drive-by-wire electric vehicle, which accomplished by the model prediction control (MPC) in a receding horizon fashion. For ensuring the dynamic stability simultaneously, the limit of stability studied by β-$\dot{\beta}$ phase plane is introduced as unequal constraints. Subsequently, pointing to the full drive-by-wire electric vehicle, the desired motion for following reference path is realized hierarchically. The results of simulations verified that the presented controller can effectively ensure the dynamic stability without compromising the tracking performance, and the theory evidence for stable path tracking is provided additionally.

Pointing to dynamic stability guarantee, this study only considers the vehicle longitudinal velocity and road friction while achieving the dynamic stability region. In the future, the more factors affected the dynamic stability region should be taken into account, such as wheel steering angles.

References

[1] K. C. Dey, L. Yan, X. Wang, et al.,"A Review of Communication, Driver Characteristics, and Controls Aspects of Cooperative Adaptive Cruise Control (CACC)," *IEEE Transactions on Intelligent Transportation Systems*, vol. 17, no. 2, pp. 491-509, 2016.

[2] Y. Guo, Z. Yu, and H. Shi, "Effects of rail thermal stress on the dynamic response of vehicle and track," *Vehicle System Dynamics*, vol. 51, no. 1, pp. 30-50, 2015.

[3] R. Marino, S. Scalzi, P. Tomei, et al., "Fault-tolerant cruise control of electric vehicles with induction motors," *Control Engineering Practice*, vol. 21, no. 6, pp.860-869, 2013.

[4] E. Lucet, R. Lenain and C. Grand, "Dynamic path tracking control of a vehicle on slippery terrain". *Control Engineering Practice*, 2015, 42:60-73.Y. Yorozu, M. M.

[5] W. Kim, D. Kim, K. Yi, et al., "Development of a path-tracking control system based on model predictive control using infrastructure sensors," *Vehicle System Dynamics*, vol. 50, no. 6, pp. 1001-1023, 2012.

[6] N. R. Kapania and J. C. Gerdes, " Design of a feedback-feedforward steering controller for accurate path tracking and stability at the limits of handling," *Vehicle System Dynamics*, vol. 53, no. 12, pp. 1687 -1704, 2015.

[7] A. Erséus, A. S. Trigell and L. Drugge, "Characteristics of path-tracking skill on a curving road," *International Journal of Vehicle Design*, vol.67, no.1, pp. 26-44, 2010.

[8] G. V. Raffo, G. K. Gomes, J. E. Normey-Rico, et al., "A Predictive Controller for Autonomous Vehicle Path Tracking," *IEEE Transactions on Intelligent Transportation Systems*, vol. 10, no. 1, pp.92-102, 2009.

[9] B. Li, H. Du and W. Li, "A Potential Field Approach-Based Trajectory Control for Autonomous Electric Vehicles With In-Wheel Motors,". *IEEE Transactions on Intelligent Transportation Systems*, vol. 18, no. 8, pp. 2044-2055, 2017.

[10] B. Gutjahr, L. Gröll and M. Werling, "Lateral Vehicle Trajectory Optimization Using Constrained Linear Time-Varying MPC," *IEEE Transactions on Intelligent Transportation Systems*, vol. 18, no. 6, pp.1586-1595, 2017.

[11] Z. Leng and M. A. Minor, "Curvature-Based Ground Vehicle Control of Trailer Path Following Considering Sideslip and Limited Steering Actuation," *IEEE Transactions on Intelligent Transportation Systems*, vol. 18, no. 2, pp. 332-348, 2017.

[12] S. I. Sakai, H. Sado and Y. Hori, "Dynamic driving/braking force distribution in electric vehicles with independently driven four wheels," *Electrical Engineering in Japan*, vol. 138, no. 1, pp. 79-89, 2002.

[13] T. Chung and K. Yi, "Side slip angle based control threshold of vehicle stability control system". *Journal of Mechanical Science & Technology*, vol. 19, no. 4, pp.985-992, 2005.

[14] H. Zhang, X. S. Li, S. M. Shi et al., "Phase Plane Analysis for Vehicle Handling and Stability," *International Journal of Computational Intelligence Systems*, vol. 4, no. 6, pp.1179-1186, 2011.

[15] P. Song, M. Tomizuka, C. F. Zong, "A novel integrated chassis controller for full drive-by-wire vehicles," *Vehicle System Dynamics*, vol. 53, no. 2, pp. 215-236, 2015.